polysaccharides

MDPI

Article

Preparation of Chitosan-Pectin-Alginate Films Reinforced with Garlic Husk (GH) Particles

Monserrat G. Escobar-Medina [1], Claudia E. Ramos-Galván [1], Cynthia G. Flores-Hernández [2], María Yolanda Chávez-Cinco [1] and J. Luis Rivera-Armenta [1,*]

[1] Centro de Investigación en Petroquímica, Instituto Tecnológico de Ciudad Madero/Tecnológico Nacional de México, Pról. Bahía de Aldair y Ave. de las Bahías, Parque de la Pequeña y Mediana Industria, Altamira 89603, Tamaulipas, Mexico

[2] Departamento de Ciencias Básicas, Tecnológico Nacional de México/Instituto Tecnológico de Querétaro, Av. Tecnológico s/n Esq. Gral. Mariano Escobedo, Col. Centro Histórico, Santiago de Querétaro 76000, Querétaro, Mexico

* Correspondence: jlriveraarmenta@itcm.edu.mx; Tel.: +52-833-5342961

Abstract

Garlic (*Allium sativum*) has antimicrobial and antioxidant properties. However, only the cloves are used from the bulb; the peels or husks are waste material with limited utility that nevertheless retain properties that can be exploited in other materials such as edible films or coatings. Chitosan is a widely used biopolymer, due its interesting properties. The same is true for alginate and pectin, which are polysaccharides that have interesting application areas; among the most common are film or coating materials in the food industry. Therefore, in this research, comprising the elaboration of films based on Chitosan-Pectin-Alginate (Q-P-A) reinforced with garlic husk (GH) particles, the films were characterized by Brookfield viscosity (the biopolymers solutions), Fourier Transform infrared Spectroscopy (FTIR), Dynamic mechanical analysis (DMA), and thermogravimetry (TGA). According to the results, the addition of GH caused a significant decrease in viscosity without altering the pseudoplasticity behavior and also generating physical interactions with the matrices; no chemical reaction byproducts were identified by FTIR. An increase in the reinforcing effect was identified in Q-GH films, whereas the opposite effect was observed in Q-P-A-GH films. In addition, no significant changes in the thermal stability were observed.

Keywords: edible films; garlic husk particles; biopolymers; composite; natural filler

Check for updates

Academic Editor: Vasiliki (Viki) Evageliou

Received: 2 February 2026
Revised: 8 March 2026
Accepted: 22 April 2026
Published: 26 April 2026

Copyright: © 2026 by the authors. Licensee MDPI, Basel, Switzerland. This article is an open access article distributed under the terms and conditions of the Creative Commons Attribution (CC BY) license.

1. Introduction

The use of biomaterials for the production of films and coatings in the food industry has gained significant interest in recent years. Once a crop is harvested, it begins to deteriorate rapidly, creating a strong need for natural packing materials capable of extending the shelf life of fruits and vegetables. Edible films and coatings are of great importance, as their main purpose is to extend shelf life and/or enrich food products. Their role is to provide a semipermeable barrier to moisture, gases, and solutes, thereby reducing respiration, moisture loss, and enzymatic browning reactions [1,2]. The main difference between edible films and edible coatings lies in the way they are applied: edible films are formed separately from the food and are later used to cover it, whereas edible coatings are formed directly on the surface of the food and must be prepared from polymers that are edible for humans, such as lipids, polysaccharides, and proteins, among others [3,4].

Chitosan, the second most abundant natural biopolymer after cellulose, is obtained from chitin through chemical, electrochemical or enzymatic methods. It is used in edible films due to its high biodegradability, low cost, good film-forming ability and antimicrobial activity against bacteria and fungi. However, its low elasticity and a certain degree of brittleness have led to the development of systems with other biopolymers and/or natural additives to enhance functionality [5,6]. Tripathi et al. [7] reported successfully compatibility of chitosan in a matrix based on chitosan/polyvinyl alcohol/pectin, reporting the formation of polyelectrolyte complexes between pectin and chitosan because of a more stable polymeric network due to electrostatic interactions. Also, the systema exhibited good antimicrobial activity, opening the opportunity to further study ternary matrices based on chitosan. In another study, chitosan was combined with alginate, and it was reported that the molecules are biocompatible and similarly generate electrostatic interactions. However, an excess of these interactions leads to the formation of structural agglomerates and fibrillar structures, resulting in pore formation. These pores, in turn, affect the mechanical properties and water vapor permeability [8].

Alginate (A) is an anionic polysaccharide found in the cell walls and intercellular regions of brown algae known as Phaeophyceae. It is composed of blocks of β-D-mannuronic acid and α-L-guluronic acid, linked by 1–4 bonds [9]. Its industrial use is focused on the production of biopolymeric films for packaging systems, due to the growing concern over the use and disposal of packaging materials (fruits, vegetables and meats) as well as its behavior as binder [10,11]. Although alginate films have low resistance to moisture, their ability to absorb it slows down food dehydration [12,13]. Due to the limitations of the chitosan/alginate matrix, the interaction of essential oils within binary matrices of these biopolymers has been explored, showing that the addition of these bioactive compounds can modify the mechanical, optical, and barrier properties of the films [14]. Pectin (P) is one of the main components of plant cells and accounts for almost one third, on a dry basis, of the cell wall of the peels of various fruits. Only a few plants are used as raw materials for the commercial production of pectin; among them are apples and certain citrus fruits. Its structure is composed of three polysaccharide domains: homogalacturonans, rhamnogalacturonan I, and rhamnogalacturonan II; however, homogalacturonan is the main component of pectin polysaccharides [15]. Their gelling capacity has enabled their development as a source of raw material for edible films and coatings in recent years. The main reason is that they exhibit good gas permeability properties; however, as a drawback, they present low water barrier performance. In addition, the combination with polysaccharides such as alginate promotes the formation of continuous, homogeneous, and pore-free films [13].

Garlic is a seasoning that has been widely used as a flavoring and antioxidant due to its attributes in food and medicine; however, its processing generates large amounts of waste (GH), which represent between 22 and 27% by weight of the total mass. This type of material has no industrial or commercial application, as it is only used as compost. Nevertheless, GH is a material rich in cellulose (approximately 43 wt %), lignin (approximately 36 wt%), hemicellulose (aprox. 22 wt%), and extractives around 3 wt% [16,17]. Recently, our research group focused on seeking applications as an additive in polymer matrices for composite materials [18]. Also, there are some reports on the use of GH, such as those by Babita et al. [19], who prepared food packaging based on chitosan. They found that the presence of particles strengthens the intermolecular interactions between the phenolic groups and the hydroxyl/amino groups of chitosan, limiting the water–chitosan interaction and decreasing water permeability. Mechanically, GH extracts led to an increase in mechanical properties, attributing this improvement to the attraction between chitosan groups and anthocyanins. Salim et al. [20] studied the addition of cellulose nanocrystals (CNC) and garlic husk extract (GH) as fillers in chitosan films. Although the transparency

of the films was affected, they observed improved mechanical properties and no significant changes in thermal stability. Furthermore, the presence of GH particles inhibited the growth of *Escherichia coli*, *Streptomyces griseorubens*, and other microorganisms. According to the above, in addition to the fact that there are no reports of the inclusion of GH in ternary matrices, this material can be used and studied as a natural reinforcement for edible films due to the good interaction with polysaccharides, seeking to improve mechanical and thermal properties as well as antimicrobial activity.

In the present work, the preparation of alginate–pectin–chitosan (Q-P-A) based films reinforced with GH is reported. The films were prepared using the casting method, adding GH at three levels: 0.01, 0.05, and 0.1%wt. The dynamic viscosity behavior of the biopolymers solutions was evaluated using a Brookfield viscometer, and the films were subsequently characterized by thermogravimetric analysis (TGA) to assess the effect of GH particles on thermal stability. Their viscoelastic properties were evaluated by dynamic mechanical analysis (DMA), and Fourier transform infrared spectroscopy (FTIR) was performed to identify functional groups and possible reactions.

2. Materials and Methods

2.1. Materials

The outer and inner husks of white garlic (*Allium sativum*), as shown in Figure 1, were obtained from a household located in Ciudad Madero, Tamaulipas. For film preparation, shrimp shell chitosan with a 75% degree of deacetylation (powder, insoluble in water, solubility of 10 mg/mL in acetic acid glacial (Sigma Aldrich, St. Louis, MO, USA), light yellow color, Sigma-Aldrich), apple pectin (powder, solubility of 0.02 g/10 mL in water, light yellow color, 74% dry basis, Sigma Aldrich), and sodium alginate (powder, derived from brown algae, white to beige color, Sigma-Aldrich), and glycerol (Sigma Aldrich) were used.

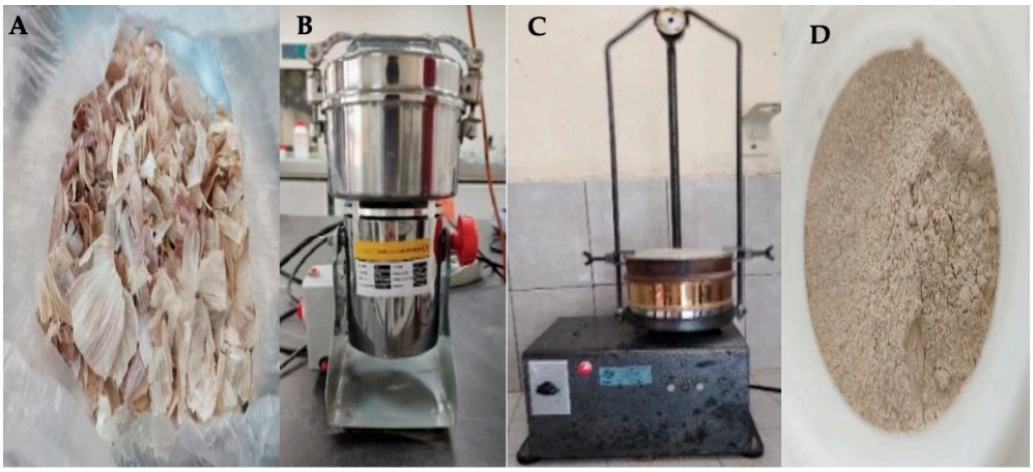


Figure 1. GH particle treatment: (**A**) GH aspect, (**B**) milling, (**C**) sieve, and (**D**) GH particles.

The GH was cleaned by removing the stalks and leaving only the "skin" of the peel, washed with distilled water, and dried in an oven at 40 °C for 24 h. They were then ground to obtain the smallest possible particle size and finally sieved using a #270 mesh to obtain particles of 53 mm. The material was identified as GH particles. Figure 1 shows the garlic husks, mill and final GH particles.

2.2. Film Preparation

The film preparation was carried out using the following procedure: solutions of each biopolymer used—chitosan (Q), pectin (P), and alginate (A)—were prepared at a concentration of 2%w/v. The solvents used were distilled water for P and A and concentrated acetic acid for Q. The solutions were mixed at 60 °C for 2 h until complete solubilization and a homogeneous appearance were achieved, using mechanical stirring at 600 rpm. Once the solutions of each biopolymer were obtained, two study matrices were selected: pure Q and Q-P-A. For the ternary matrix, equal proportions of each biopolymer were mixed following an order of addition that consisted of keeping the chitosan under constant stirring while gradually adding the proportions of pectin and alginate.

The addition and mixing of the GH particles were carried out at room temperature without applying heat, to prevent biopolymer degradation and solvent evaporation, using mechanical stirring at 600 rpm. Additionally, during this mixing process, glycerol was added at a concentration of 0.5%wt. After obtaining a homogeneous appearance, equal volumes of 30 mL were poured into 9 cm diameter glass Petri dishes. Finally, the films were allowed to dry until complete solvent evaporation under controlled temperature and humidity conditions (23 °C ± 2 and 44% ± 3 relative humidity) for 4 days. The proportions of each polymer used and the codes assigned to each material are reported in Table 1. The GH concentrations used in this study were determined based on preliminary tests in which higher concentrations were evaluated. However, these concentrations did not allow proper film formation, so they were adjusted to levels that ensured correct appearance and homogeneity.

Table 1. Films prepared and ratios and codes for films prepared.

Material	**Garlic Husk Particles (%wt)**		
	0.01	0.05	0.1
Q	Q-GH 0.01	Q-GH-0.05	Q-GH 0.1
Q-P-A	Q-P-A GH 0.01	Q-P-A GH 0.05	Q-P-A GH 0.1

2.3. Film Characterization

2.3.1. Dynamic Viscosity

The rotational viscosity of the biopolymer solutions (before pouring into the Petri dish for drying) was determined prior to film formation. Viscosity was measured by determining the torque required to maintain a constant rotational speed of a cylindrical spindle while it was immersed in the solution at a constant temperature. The measured torque is directly related to the viscosity of the sample. The measurements were carried out using a Brookfield DV-II+Pro instrument (Middleboro, MA, USA) equipped with a Thermocell heating system, employing a SC4-21 spindle geometry [13,14]. The sample size for this spindle was 8.0 g, and viscosities were measured at 25 and 60 °C over a speed range of 2 to 100 rpm, reporting the viscosities in centipoise (cP).

During the analysis, potential sources of experimental error were considered, such as temperature fluctuations and variations in the rotational speed of the spindle. Therefore, the samples were allowed to reach thermal equilibrium (25 °C and 60 °C) prior to the measurements, using a digital thermocouple thermometer to verify the temperature and avoid variations in the rheological response. For each shear rate (rpm), the readings were recorded over a 30 s interval in order to standardize the measurement time and allow stabilization of the torque generated by the system before recording the final viscosity value. To ensure the reproducibility and reliability of the results, three independent replicates were performed for each shear rate, and the corresponding average value was subsequently calculated.

2.3.2. FTIR Spectroscopy

This type of analysis was performed to identify the functional groups of the materials used in film preparation and any new functional groups that might indicate interactions among them. The analyses were carried out for the obtained films using a PerkinElmer Spectrum One FTIR instrument (Springfield, IL, USA) equipped with an ATR accessory with a ZnSe crystal, over a range of 4000 to 600 cm^{-1}, with 12 scans and a resolution of 4 cm^{-1}.

2.3.3. Dynamic Mechanical Analysis (DMA)

This technique was chosen to analyze, as a function of temperature and time, the deformation of the films obtained and the resulting force transmitted through them, and to use the obtained information to compare their mechanical and viscoelastic behavior. For this analysis, TA Instruments DMA Q-800 equipment (New Castle, DE, USA) was used, equipped with an ACS-3 cooling system and a film-type clamp. The films were cut, and the sample dimensions were 30 × 10 × 0.15 mm, with a temperature range of –50 to 180 °C and a heating rate of 5 °C/min.

2.3.4. Thermogravimetric Analysis (TGA)

The TGA analysis was performed to evaluate the thermal stability of the materials and to identify the weight loss behavior of the prepared films. For this purpose, a TA Instruments Q600 simultaneous thermal analyzer (SDT) (New Castle, DE, USA) was used under a nitrogen atmosphere with a flow rate of 100 mL/min, over a temperature range from ambient to 700 °C, with a heating rate of 10 °C/min, using a platinum crucible and a sample amount of 10 mg of the films.

3. Results

3.1. Dynamic Viscosity

The dynamic viscosity is important for understanding how the materials flow in solution, as gel formation depends on the concentration, which also is associated with compatibility of the polysaccharides in combination [15]. Tables 2 and 3 presents the viscosity value of solutions before the preparation of films at different speeds. It is evident that when GH particles are added to control solutions, the viscosity values decrease in both matrices. Also, a pseudoplastic behavior is observed and, at high shear rate, tends to maintain a non-Newtonian behavior [8,16]. For the Q-GH films, at high shear rates, the control and the solution with 0.01 GH exhibited a torque that exceeded the limit (90%), whereas at low shear rates, in most of the solutions, the torque was below 10%, meaning the values were not representative.

Solutions of chitosan, pectin, and alginate alone tend to exhibit pseudoplastic behavior at the concentrations used in this study; therefore, the only effect produced by the GH particles in the solutions is a drastic decrease in viscosity as the concentration increases. This effect can be attributed to the presence of lignin and flavonoids, which are major components of plant peels and contain phenolic groups. According to Tudorache et al. [17], these phenolic components affect rheological properties by decreasing viscosity and pseudoplastic behavior as the shear rate increases. This occurs because, after complexation with polysaccharides, aggregates are formed that tend to exhibit more interactions between molecules within the aggregates, leading to a reduced ability to increase their viscosity.

Table 2. Dynamic viscosity results of Q-GH Films.

	Dynamic Viscosity, cPoise							
RPM	**Q**		**Q-GH 0.01**		**Q-GH 0.05**		**Q-GH 0.1**	
	25 °C	60 °C	25 °C	60 °C	25 °C	60 °C	25 °C	60 °C
2	1483	184	1275	**	**	**	**	**
5	1270	170	1112	**	**	**	**	**
10	1155	155	975	149	365	**	**	**
20	1018	153	780	128	331	119	**	**
30	972	142	771	112	287	94	133	**
50	826	136	690	99	235	86	94	60
60	**	131	653	93	182	72	70	48
100	**	101	**	88	166	66	62	39

** Samples not reporting viscosity.

In the case of temperature, this can be explained according to previous works that report that an increase in temperature generates an increase in molecular distances due the weakening of intermolecular forces. Furthermore, the particle–particle interactions decrease, and and increase in shear rate causes particles to be oriented in the flow direction and break the reticular structure of polysaccharide molecules, thus decreasing flow resistance [18].

Table 3. Dynamic viscosity results of Q-P-A-GH films.

	Dynamic Viscosity, cPoise							
RPM	**Q-P-A**		**Q-P-A GH 0.01**		**Q-P-A GH 0.05**		**Q-P-A GH 0.1**	
	25 °C	60 °C	25 °C	60 °C	25 °C	60 °C	25 °C	60 °C
10	996	948	904	860	871	731	824	662
20	957	869	917	798	845	654	792	602
30	907	790	871	726	799	611	765	548
50	877	767	829	689	764	553	688	483
60	850	705	775	636	722	520	618	461
100	845	694	741	619	631	515	602	457

The addition of GH particles results in decreasing viscosity; the low viscosity could be beneficial because, with high viscosity, spreading is not easy and manipulation is difficult, causing a thickening of films [19].

Figure 2 shows the appearance of the synthesized films. For the Q-GH matrix, the addition of GH did not significantly affect the color or opacity, showing a homogeneous and smooth surface to the touch. For the Q-P-A-GH matrix, a yellow-brown coloration was observed, which can be attributed to two factors. On one hand, pure pectin has a slight yellowish color, which could affect the appearance of the final solution; this could also be due to pectin's tendency to influence the internal structure of the films, as its less-organized structure reduces the protective barrier against UV rays, promoting the decomposition of lignin present in GH, which is susceptible to degradation by heat or sunlight [12,20]. In general, films are flexible, and the good dispersion of GH particles is evident, as the presence of particles in the films can be observed. However, the antimicrobial effect was not investigated in the present study; therefore, complementary studies are suggested to evaluate this aspect in relation to the presence of GH.

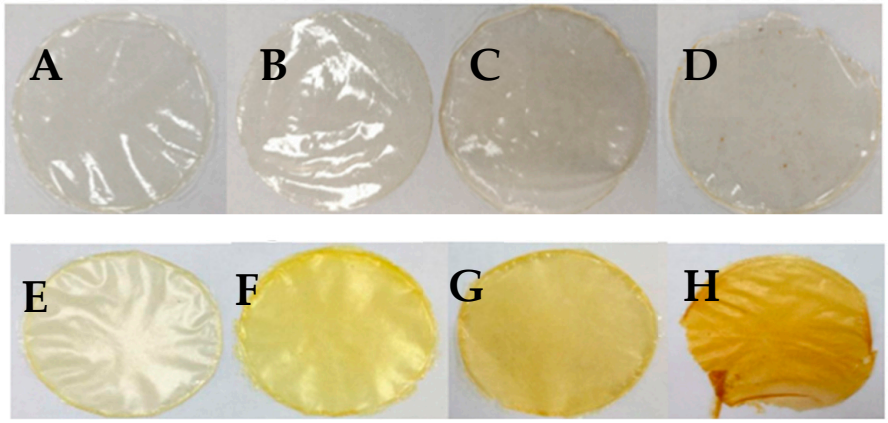


Figure 2. Appearance of films: (**A**) Q, (**B**) Q-GH 0.01, (**C**) Q-GH 0.05, (**D**) Q-GH 0.1, (**E**) Q-P-A, (**F**) Q-P-A GH 0.01, (**G**) Q-P-A GH-0.05, and (**H**) Q-P-A GH-0.1.

3.2. FTIR Spectroscopy

Figure 3 shows the FTIR spectrum of GH, where the main signals can be identified as follows: 3238 cm^{-1}, corresponding to signals attributed to O–H bond stretching, characteristic of polysaccharides such as cellulose, one of the main components of garlic husks; 2981 and 2919 cm^{-1}, associated with asymmetric and symmetric vibrations of CH_2 and CH_3 groups, present in the structure of cellulose, hemicellulose, and lignin, polysaccharides found in GH [20–29]. The peak at 1743 cm^{-1} is attributed to the C=O stretching of acetylsalicylic groups attached to the aromatic ring of lignin and hemicellulose structures. The peak at 1600 cm^{-1} is associated with C=C bonds of the aromatic rings present in lignin and flavonoids. Other characteristic cellulose peaks appear at 1148, 1096, and 1007 cm^{-1}, corresponding to the C–O–C group [30–32]. On the other hand, the peaks at 1236, 1044, and 720 cm^{-1} are associated with the C=S, S=O, and S=S bonds of sulfur-containing compounds present in garlic husk. Another peak associated with sulfur presence is the peak at 1379 cm^{-1}, which is found in sulfur compounds that confer antimicrobial activity to GH particles, such as allin, allicin, diallyl disulfide, among others [33,34].

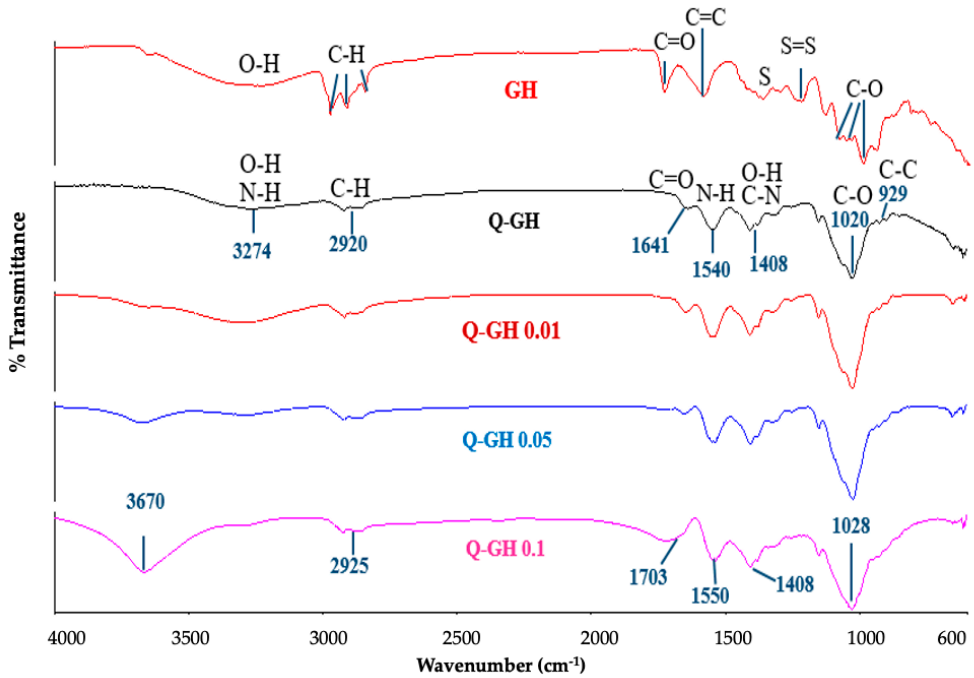


Figure 3. FTIR Spectrum of GH and Q-GH with different content of GH.

In addition, Figure 3 shows the IR spectrum of the Q and Q-GH films, where peaks can be observed at 3274 cm^{-1}, corresponding to the bending vibrations of the O–H bonds, which would be "overlapped" with the N–H bond peaks of the amide groups in their structure [5,7]. In addition, peaks at 2929 cm^{-1} are attributed to the C–H stretching vibrations of the CH_2 and CH_3 groups. The signal at 1641 cm^{-1} corresponds to the C=O stretching, which is associated with acetyl groups that were not completely removed (the chitosan used has a 75% degree of deacetylation) [3]. The peaks at 1408 and 1020 cm^{-1} are attributed to C–N and C–O stretching vibrations of the primary amino group and the pyranose ring [35].

The addition of GH did not generate new peaks; therefore, it is established that there is no chemical interaction with the chitosan matrix. Only physical interactions are present, which can be identified by the increase and shift of the peaks associated with the O–H and N–H groups (3670 cm^{-1}) as well as the peaks at 1550 and 1408 cm^{-1} associated with chitosan amide groups [20]. These interactions may correspond to hydrogen bonding between Q molecules and the phenolic groups of the GH particles, as previously suggested in the viscosity analysis. These peaks are like those reported in previous studies, which indicate that pure chitosan exhibits peaks at 1633 and 1530 cm^{-1}, as well as at 1400 cm^{-1}, attributed to the C=O (amide I) and N–H (amide II) groups [36].

On the other hand, Kaya et al. [37] reported that one way to identify strong intermolecular interactions between phenolic compounds and chitosan is through an increase in the intensity of the amide group bands between 1549 and 1380 cm^{-1}. In addition, the O–H stretching peak is a sensitive indicator of hydrogen bond strength, exhibiting significant broadening for strong hydrogen bonds, whereas a shift toward higher frequencies is attributed to the migration of the electron cloud of oxygen atoms in the phenolic groups to higher wavenumbers [38,39].

Figure 4 shows the FTIR spectrum of the Q-P-A-GH films at different GH contents. Since this is a complex matrix composed of three base solutions, there is an overlap of bond signals from the functional groups present in its structure. The characteristic peaks of Q appear at 3256, 1640, 1405, and 1025 cm^{-1}, attributed to the O–H, N–H (CH_2), and C–O groups present in the glycosidic ring [7,8,36]. P exhibits peaks corresponding to hydroxyl, carbonyl, carboxylate, and glycosidic groups at 3260, 1740 (a characteristic signal of the C=O stretching of esterified carboxyl groups), 1653, 1400, and 1152 cm^{-1} [38]. A exhibits characteristic peaks at 2930, 1600, and 1400 cm^{-1}, corresponding to CH_2, COOH, and O–H groups, respectively, with an additional peak at 1300 cm^{-1} [24]. In the spectrum, a dominance of A-related signals over those of Q and P is observed, due to the presence of two characteristic peaks of similar intensity at 1601 and 1411 cm^{-1} [40]. Additionally, a broad and intense peak with small shoulders appears at 1025 cm^{-1}, associated with mannuronic and guluronic groups, along with a small peak at 948 cm^{-1}, attributed to C–O stretching vibrations [41].

Sibaja et al. [42] reported that in Q-A films, the FTIR spectrum showed a greater influence or dominance of A-related signals. In the present work, upon additionally incorporating a P matrix, the same dominance effect of this biopolymer was observed. Additionally, according to Prateepchanachai et al. [36], pure chitosan exhibits peaks at 1640 and 1530 cm^{-1}, corresponding to amide I (C=O stretching) and amide II (N–H bending) vibrations, which helps to confirm that chitosan is not the dominant component in this matrix. Upon the addition of GH particles, a shift of the O–H and N–H peaks toward higher wavenumbers (3364 cm^{-1}) is observed, along with a decrease in intensity and a shift of the peak at 1601 cm^{-1} toward lower wavenumber values. The first peak is associated with an increase in hydrogen bonding (physical interactions) between the molecules. This behavior, according to Sidek et al. [39], is attributed to the presence of phenolic compounds

in the garlic particles, whose availability increases as their concentration rises. On the other hand, the decrease of the peak at 1601 cm^{-1} toward lower % transmittance values may be related to reduced transparency and increased opacity of the films.

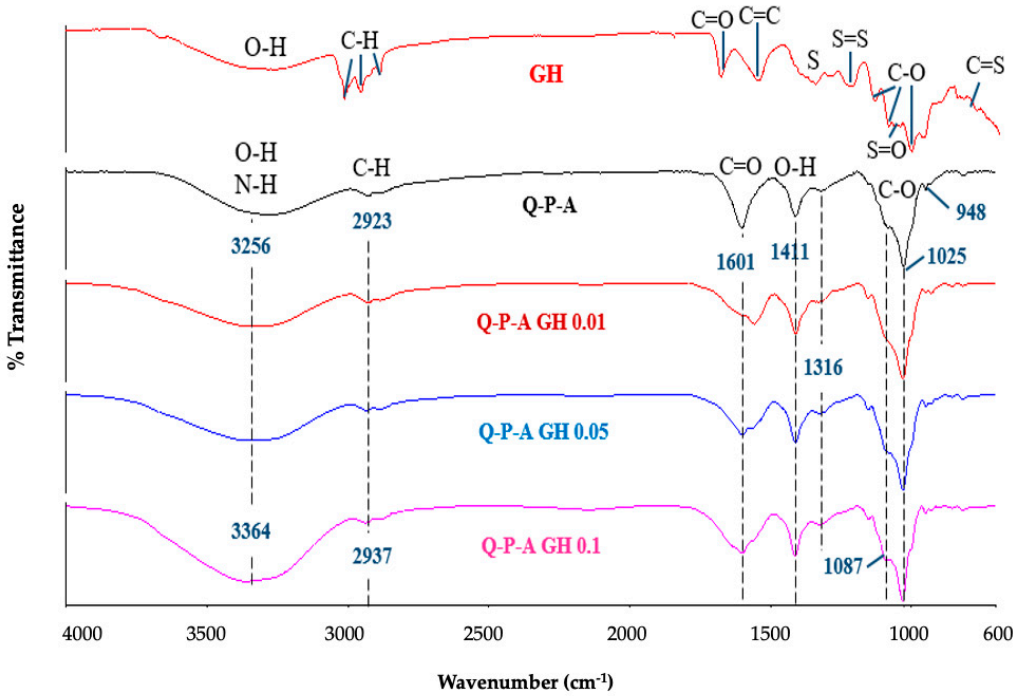


Figure 4. FTIR spectra for Q and Q-P-A-GH with different content levels of GH.

Overall, no peaks associated with compounds formed through chemical reactions were observed; only changes in peak intensities and shifts were identified, which are attributed to physical interactions between the molecules and the GH particles.

3.3. Dynamic Mechanical Analysis (DMA)

Figure 5 shows the DMA thermogram of Q-GH films, in which it can be observed that as temperature increases, the storage modulus decreases in value, indicating the transition from a rigid to a soft state. Additionally, three main regions can be identified: the first region is associated with molecular motions due to localized movements or secondary chain motions related to free volume; the second region corresponds to the glass transition of the material; and finally, a region in which an increase in the storage modulus (E′) is observed, which is attributed to the rapid alignment of polymer chains under sinusoidal stress, generating a plasticizer-like effect [43].

On the other hand, it was observed that the addition of GH increased the storage modulus values in the Q-GH films, except for the film containing 0.05 GH, which exhibited the lowest E′ value at low temperatures; this indicates that the modified films tend to be more rigid. In addition, at temperatures above 30 °C, the effect of GH addition becomes evident, as increasing particle content leads to a higher E′ compared to pure Q. This behavior confirms a reinforcing effect of the GH particles on the Q matrix, resulting in a stiffer material. Among the basic requirements for edible films, mechanical properties stand out, since low resistance can cause cracking or premature failure of the fruit during production, handling, storage or use [44]. This effect is beneficial, as it has been reported that a major limitation of chitosan-based films is their low mechanical properties compared to plastic films [45]. This effect is attributed to the presence of particles that restrict the molecular mobility of Q chains, which is associated with interfacial adhesion between the particles and the Q matrix and is simultaneously linked to hydrogen bonding interactions

identified by FTIR [46,47]. There are reports indicating that increased interactions between molecules of certain additives (antioxidants) containing phenolic groups lead to an increase in the storage modulus (E′) in chitosan matrices, as observed in the present work [48,49].

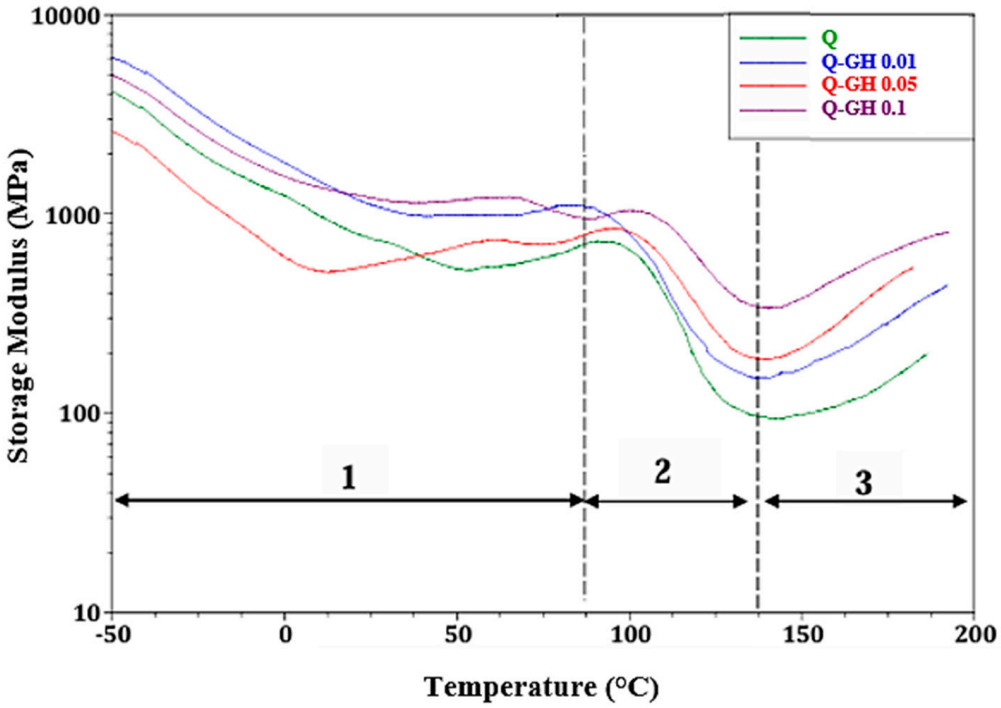


Figure 5. DMA thermogram for Q-GH films.

On the other hand, the DMA thermogram for Q-P-A films reinforced with GH is shown in Figure 6, indicating that the storage modulus decreases in the GH-reinforced films compared to the unreinforced film. Only the film with the highest GH content (0.1%) shows a higher modulus value at low temperatures (below 50 °C), an effect that could be improved by the addition of a crosslinking agent that would strengthen the network interactions between the polysaccharide chains. The crosslinking agent, by reinforcing the bonds between polymer chains, can improve the barrier against UV light and thereby reduce the degradation of the lignin present in the brownish-colored films.

Galus et al. [28] reported that the presence of pectin tends to affect the internal structure of this type of films by reducing their mechanical strength, which could explain a similar behavior in this complex matrix. Similar results were reported by Kurek et al. [50], who indicated that pectin films containing powdered blackcurrant residues exhibited a decrease in the storage modulus value. In addition, they mentioned the presence of discontinuities in the films due to a lack of cohesion between the polymer chains, which increased chain mobility and reduced their mechanical strength.

Therefore, the lack of cohesion is attributed to P, which tends to affect the internal structure of the films by promoting a less organized arrangement and generating a plasticizing effect, even when it is not present as the dominant component in the matrix [11,28]. Some studies report that the addition of antioxidant agents such as ferulic acid (polyphenols) to Q-A films results in an increase in mechanical properties [51]. However, for this matrix, the presence of P affected the molecular ordering, preventing an increase in the storage modulus.

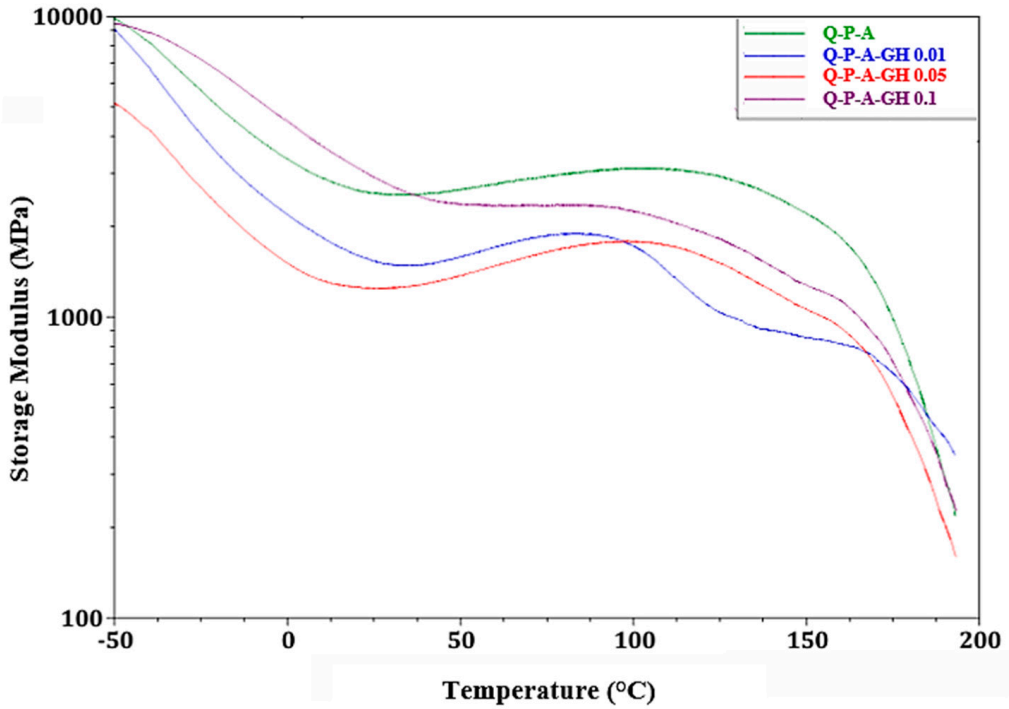


Figure 6. DMA thermogram of Q-P-A-GH films.

On the other hand, although secondary interactions such as hydrogen bonding contribute to the structural cohesion of edible films, it is believed that an excess of these interactions leads to disorganization within the biopolymer network. Competition for active sites between GH and the hydroxyl, amino, and carbonyl groups in the base solutions Q, P, and A within the ternary complex matrix, as well as the formation of highly associated domains, reduced structural uniformity, thereby affecting the mechanical properties.

This is supported by reports indicating that the complex interaction between polyphenols and polysaccharides such as Q, P, and A impacts the structure and molecular organization of the system, which may modify its functionality [52–54]. This effect mainly depends on the concentration and intrinsic properties of the polyphenol [55].

However, further research is still required to better understand the structural changes and underlying mechanisms involved and to evaluate the possible antimicrobial effect generated by the presence of GH. Such knowledge will be crucial for the development of innovative systems for food preservation, particularly for fruits and vegetables.

3.4. Thermogravimetric Analysis (TGA)

Thermogravimetric analysis allows the evaluation of the thermal stability of materials by monitoring weight as a function of temperature. Figure 7 shows the TGA thermogram of garlic, in which three weight-loss stages characteristic of lignocellulosic materials are observed [51]. The first weight-loss stage, with a degradation temperature of 157 °C in the DTG curve, is attributed to the evaporation of bound water, mainly associated with hydroxyl groups in the amorphous phase, as well as volatile compounds [20]. In the second and main weight-loss stage (65 wt%), two decomposition processes occur at 242.5 °C and 348 °C, associated with the degradation of hemicellulose and pectin, as well as cellulose and lignin, respectively. Finally, above 430 °C, a slow weight loss is observed, indicating the formation of carbonaceous material, which results in a residue of approximately 20 wt% [32,56].

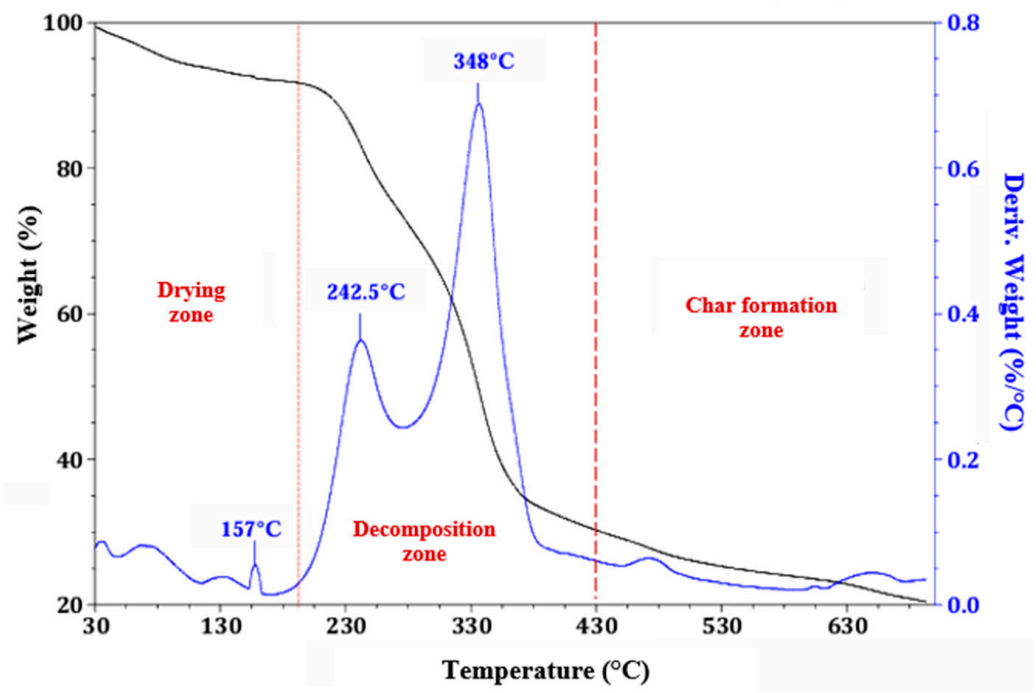


Figure 7. TGA/DTG thermogram of GH particles.

According to Moreno et al. [56], the degradation of cellulosic materials begins at 150 °C and continues up to 380 °C, during which decarboxylation, depolymerization, and decomposition into cellulose, hemicellulose, and lignin fragments occur. Therefore, cellulosic materials degrade below 400 °C, and the degradation temperature depends on the structure and chemical composition of the material, as well as on the region where the process takes place. However, other studies have reported that lignin exhibits a broad degradation range due to its complex and aromatic structure. Therefore, its decomposition can extend from 200 °C to above 500 °C, with most of the degradation occurring around 478 °C and residues remaining beyond this temperature. For this reason, the lignin decomposition signal may overlap with that of cellulose [57].

Figure 8A shows the weight-loss thermogram as a function of temperature for Q-GH films, in which three decomposition stages can be identified. The first stage, occurring between 30 °C and 130 °C, is attributed to the evaporation of free and bound water, as well as solvent residues (residual acetic acid). The second stage occurs between 130 °C and 230 °C, where a weight loss of approximately 25–30% is observed and is associated with the degradation of the glycerol used in the formulation [19,37,58]. The main weight loss, around 40–60%, occurs between 230 °C and 330 °C, corresponding to the deacetylation, decarboxylation and thermal decomposition of the Q structure and GH.

This behavior is consistent with previous studies reporting the decomposition of the carbohydrates, hemicellulose, and cellulose of Q films at approximately 223 °C and 326 °C [19,20]. In addition, Soni et al. [59], reported that chitosan exhibits an initial decomposition stage around 100 °C, corresponding to the evaporation of absorbed water, acetic acid, and volatile compounds. Furthermore, the major weight loss is attributed to structural degradation and thermal decomposition, occurring between 220 and 380 °C. At the end of the temperature range, the presence of residues represents char formation, where the destruction of the crystalline regions and the decomposition of lignin and cellulose residues from Q and GH occur. This is followed by the incomplete elimination of dispersed atoms such as carbon, oxygen, and hydrogen, resulting in the formation of carbonaceous material.

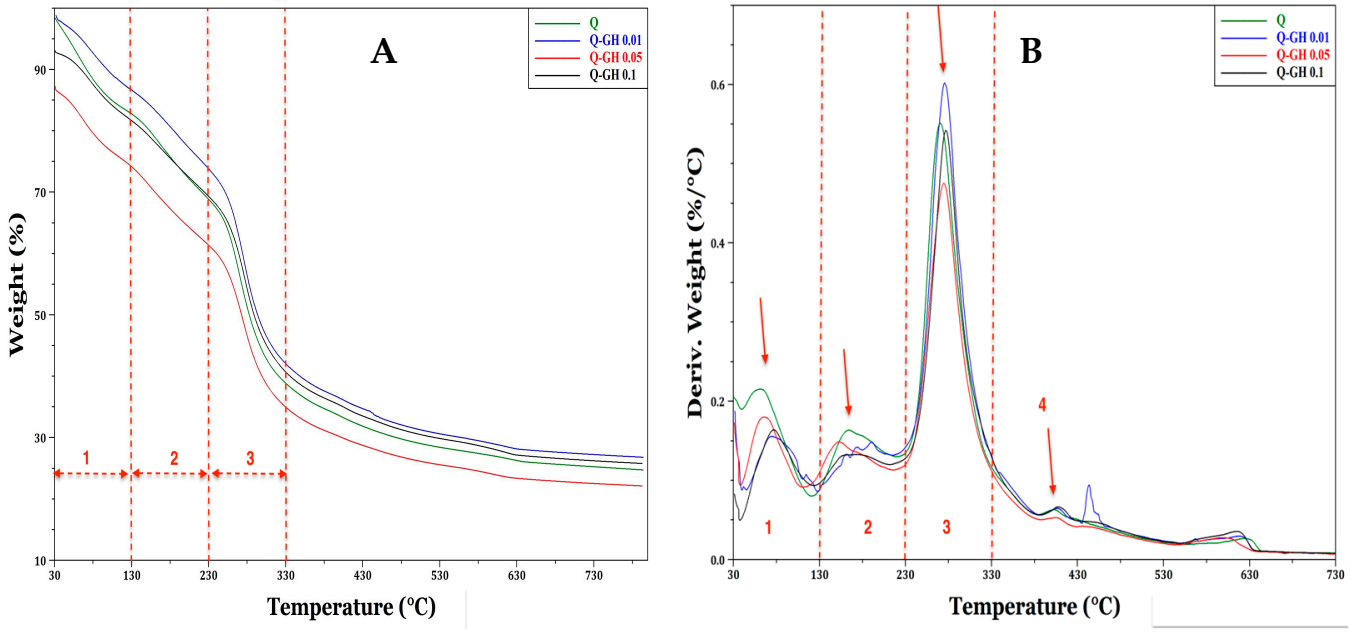


Figure 8. TGA weight loss thermogram (**A**) and derivative weight loss thermogram (**B**) of Q-GH films.

In Figure 8B, the derivative weight-loss curves can be observed, in which the previously mentioned decomposition stages are more clearly defined. Additionally, it is suggested that the fourth, smaller peak at an approximate temperature of 400 °C corresponds to the decomposition of lignin residues from the GH particles, as Alzagameem et al. reported [57].

It is observed that the peak intensity is lower for the GH-reinforced films, which is associated with a lower decomposition rate. However, this reinforcing effect is not very pronounced, suggesting the preservation of thermal stability without significant alterations. Furthermore, no additional signals indicative of secondary reaction products were observed within the matrix.

For the Q-P-A-GH films, three weight-loss stages were once again observed, according to Figure 9A, B. The first weight loss (10–20%) occurs in the temperature range from 30 °C to 110 °C, the second weight loss (20–30%) is observed between 110 °C and 200 °C, while the stage of highest decomposition (30–60%) occurs approximately from 200 °C to 270 °C. The first weight loss is attributed to the evaporation of water and solvents, the second is associated with the degradation of rings and functional groups of the alginate and glycerol chains, whereas in the third stage, the chitosan and alginate structures mainly degrade and decompose. This stage is attributed to the decomposition of the chitosan backbone along with the cleavage of deacetylated units, as well as the pyrolytic decomposition and degradation of galuronic and mannuronic acid chains. The presence of pectin is associated with a shift of the decomposition zones toward lower temperatures [8,28,36,60].

These degradation and decomposition stages can be observed in Figure 9B by the presence of peaks at 70 °C, 170 °C, 210 °C, and 240 °C. The small shoulder at approximately 300 °C is associated with the decomposition of residues from the previous stage as well as lignocellulosic residues from GH [61]. In addition, the results show that the addition of GH improved thermal stability by exhibiting a decrease in the ratios of the derivative weight loss with respect to temperature, indicating that the modified films present a lower weight-loss rate, mainly in the temperature range from 30 °C to 110 °C [19,20]. Furthermore, no additional signals indicative of secondary reaction products were observed within this ternary matrix due to the presence of GH particles.

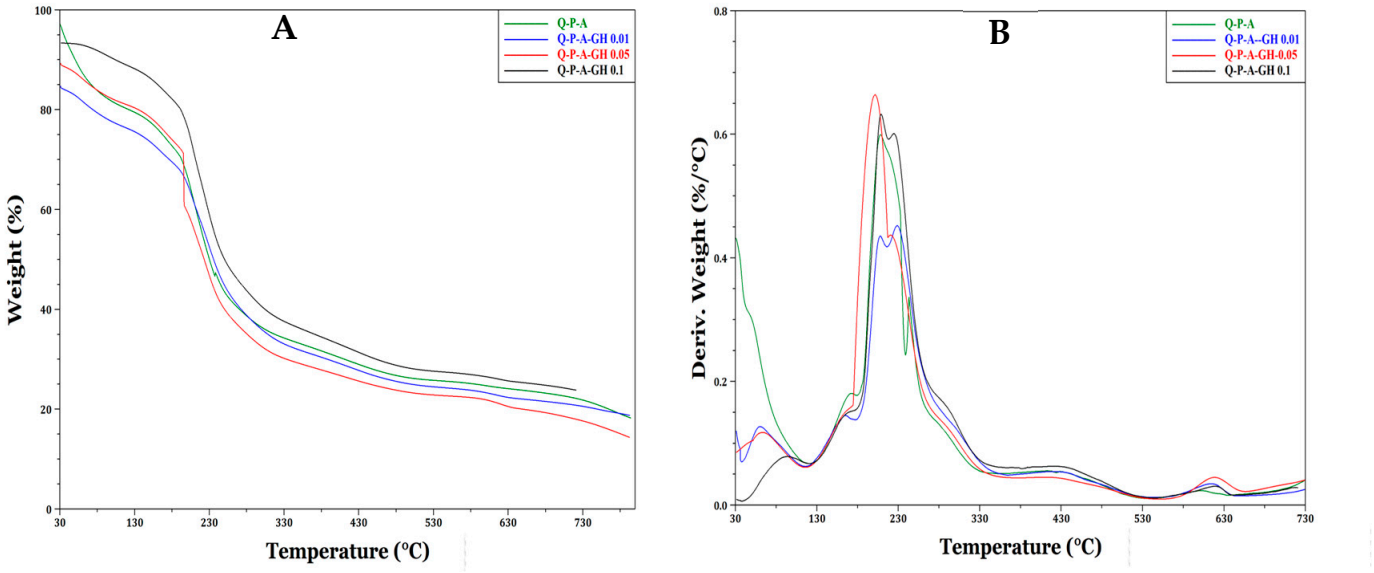


Figure 9. Bulleted lists look like this: TGA weight loss thermogram (**A**) and derivative weight loss thermogram (**B**) of Q-P-A-GH films.

4. Conclusions

It was possible to synthesize Q- and Q-P-A-based films modified with GH particles based on a casting method, exhibiting an appearance acceptable to consumers for application in food preservation. The addition of GH resulted in a significant decrease in viscosity, which was attributed to the aggregates formed after complexation with polysaccharides, leading to a reduced ability to increase their viscosity. This effect may be advantageous for the design of agro-industrial processes for fruits and vegetables, since an ideal coating is expected to combine good surface adhesion with low viscosity. Through FTIR analysis, the type of physical interaction (hydrogen bonding) between the polysaccharide molecules was confirmed, with no products attributed to possible chemical reactions. The GH concentration affected the appearance of the films, with those containing pectin exhibiting a brownish coloration. In addition, it was found that the presence of pectin in Q-P-A-GH films reduced the mechanical properties due to a plasticizing effect or disorganized structure in the matrix, whereas Q films showed better appearance and higher storage modulus values because of improved physical interactions between the matrix and GH.

However, the increase in thermal stability was not very pronounced, which suggests the need to study higher concentrations than those used in the present work and/or their combination with crosslinking agents to obtain suitable thermal properties for food applications. It is suggested to study the antimicrobial activity and antioxidant capacity due to the insufficient characterization, to evaluate the effect of GH within the developed biopolymer matrices. The synthesized material represents an opportunity for the development of films for the preservation of fruits and vegetables.

Author Contributions: Conceptualization, M.G.E.-M., C.E.R.-G. and J.L.R.-A.; methodology, M.G.E.-M., C.G.F.-H. and M.Y.C.-C.; software, C.E.R.-G., C.G.F.-H. and M.Y.C.-C.; validation, J.L.R.-A. and C.G.F.-H.; formal analysis, M.G.E.-M. and M.Y.C.-C.; investigation, M.G.E.-M., C.E.R.-G. and J.L.R.-A.; resources, J.L.R.-A. and M.Y.C.-C.; data curation, C.G.F.-H. and C-E-R-G.; writing—original draft preparation, M.G.E.-M. and J.L.R.-A.; writing—review and editing, M.G.E.-M. and J.L.R.-A.; visualization, M.Y.C.-C.; supervision, C.E.R.-G.; project administration, J.L.R.-A.; funding acquisition, none. All authors have read and agreed to the published version of the manuscript.

Funding: This research received no external funding.

Data Availability Statement: The original contributions presented in the study are included in the article, further inquiries can be directed to the corresponding author.

Conflicts of Interest: The authors declare no conflicts of interest.

Abbreviations

The following abbreviations are used in this manuscript:

Q	Chitosan
Q-P-A	Chitosan-Pectin-Alginate films
GH	Garlic husks
FTIR	Infrared Spectroscopy
DMA	Dynamic Mechanical Analysis
TGA	Thermogravimetric Analysis
CNC	Cellulose nanocrystals

References

1. Montalvo, C.; López-Malo, A.; Palou, E. Películas comestibles de proteína: Características, propiedades y aplicaciones. *Temas Sel. Ing. Aliment.* **2012**, *6*, 32–46.
2. Díaz-Montes, E.; Castro-Muñoz, R. Edible Films and Coatings as Food-Quality Preservers: An Overview. *Foods* **2021**, *10*, 249. [CrossRef]
3. Ortega Cardona, C.E.; Aparicio Fernández, X. Quitosano: Una alternativa sustentable para el empaque de alimentos. *Rev. Digit. Univ.* **2020**, *21*, 6. [CrossRef]
4. Suhag, R.; Kumar, N.; Trajkosva-Petroska, A.; Upadhyay, A. Film formation and deposition methods of edible coating on food products: A review. *Food Res. Int.* **2020**, *136*, 109582. [CrossRef]
5. Butler, B.L.; Vergano, P.J.; Testin, R.F.; Bunn, J.M.; Wiles, J.L. Mechanical and Barrier Properties of Edible Chitosan Films as affected by Composition and Storage. *J. Food Sci.* **1996**, *5*, 953–956. [CrossRef]
6. Luo, Y.; Wang, Q. Recent Advances of Chitosan and Its Derivatives for Novel Applications in Food Science. *J. Food Process. Beverages* **2013**, *1*, 1–13.
7. Tripathi, S.; Mehrotra, G.K.; Dutta, P.K. Preparation and physicochemical evaluation of chitosan/poly (vinyl alcohol)/pectin ternary film for food-packaging applications. *Carbohydr. Polym.* **2010**, *79*, 711–716. [CrossRef]
8. Arzate-Vázquez, I.; Chanona-Pérez, J.J.; Calderón-Domínguez, G.; Terres-Rojas, E.; Garibay-Febles, V.; Martínez-Rivas, A.; Gutiérrez-López, G.F. Microstructural characterization of chitosan and alginate films by microscopy techniques and texture image analysis. *Carbohydr. Polym.* **2012**, *87*, 289–299. [CrossRef] [PubMed]
9. Hernández-Carmona, G.; Rodríguez-Montesinos, Y.E.; Arvizu-Higuera, D.L.; Reyes-Tisnado, R.; Murillo-Álvarez, J.I.; Muñoz-Ochoa, M. Technological advance for alginate production in Mexico. *Ing. Investig. Y Tecnol.* **2012**, *13*, 155–168.
10. Aly, A.A.; Maraei, R.W. Role of irradiated and un-irradiated alginate as edible coating in physicochemical and nutritional quality of cherry tomato. *BMC Plant Biol.* **2024**, *24*, 1257. [CrossRef] [PubMed]
11. Jayakody, M.M.; Vanniarachchy, M.P.G.; Wijesekara, I. Seaweed derived alginate, agar, and carrageenan based edible coatings and films for the food industry: A review. *J. Food Meas. Charact.* **2022**, *16*, 1195–1227. [CrossRef]
12. Cazón, P.; Velazquez, G.; Ramírez, J.A.; Vázquez, M. Polysaccharide-based films and coatings for food packaging: A review. *Food Hydrocoll.* **2017**, *68*, 136–148. [CrossRef]
13. Metha, C.; Pawar, S.; Suvarna, V. Recent advancements in alginate-based films for active food packaging applications. *Sustain. Food Technol.* **2024**, *5*, 1246–1265. [CrossRef]
14. Guzmán-Pincheira, C.; Moeini, A.; Oliveira, P.E.; Abril, D.; Paredes-Padilla, Y.A.; Benavides-Valenzuela, S. Development of Alginate-Chitosan Bioactive Films Containing Essential Oils for Use in Food Packaging. *Foods* **2025**, *14*, 256. [CrossRef]
15. Pérez-Espitia, P.J.; Wen-Xian, D.; Avena-Bustillos, R.J.; Ferreira-Soares, N.F.; McHugh, T. Edible films from pectin: Physical-mechanical and antimicrobial properties—A review. *Food Hydrocoll.* **2014**, *35*, 287–296. [CrossRef]
16. Reddy, J.P.; Rhim, J.W. Extraction and characterization of cellulose microfibers from agricultural wastes of onion and garlic. *J. Nat. Fibers* **2018**, *15*, 465–473. [CrossRef]
17. Reddy, J.P.; Rhim, J.W. Isolation and characterization of cellulose nanocrystals from garlic skin. *Mat. Lett.* **2014**, *129*, 20–23. [CrossRef]
18. Villalobos-Neri, E.E.; Macchlesh Del Pino-Perez, L.A.; Velasco-Ocejo, H.A.; Rivera-Armenta, J.L.; Espindola-Flores, A.C. Preparation and evaluation of thermal properties of composites based on polypropylene reinforced with garlic husk particles (GHP). *J. Nat. Fibers* **2023**, *20*, 2145409. [CrossRef]

19. Chaudhary, B.U.; Lingayat, S.; Banerjee, A.N.; Kale, R.D. Development of multifunctional food packaging films based on waste Garlic peel extract and Chitosan. *Int. J. Biol. Macromol.* **2021**, *192*, 479–490. [CrossRef]
20. Salim, M.H.; Kassab, Z.; Abdellaoui, Y.; García-Cruz, A.; Soumare, A.; Ablouh, E.H.; El Achaby, M. Exploration of multifunctional properties of garlic skin derived cellulose nanocrystals and extracts incorporated chitosan biocomposite films for active packaging application. *Int. J. Biol. Macromol.* **2022**, *210*, 639–653. [CrossRef]
21. Barreda-Molina, A.L. *Consejo Nacional de Ciencia*; Tecnología e Innovación-UNSA: Toluca de Lerdo, Mexico, 2016; pp. 42–43.
22. Prakash, A.; Baskaran, R.; Vadivel, V. Citral nanoemulsion incorporated edible coating to extend the shelf life of fresh cut pineapples. *LWT* **2020**, *118*, 108851. [CrossRef]
23. Morales-Contreras, B.E.; Wicker, L.; Rosas-Flores, W.; Contreras-Esquivel, J.C.; Gallegos-Infante, J.A.; Reyes-Jaquez, D.; Morales-Castro, J. Apple pomace from variety "Blanca de Asturias" as sustainable source of pectin: Composition, rheological, and thermal properties. *LWT* **2020**, *117*, 108641. [CrossRef]
24. Gómez-Díaz, D.; Navaza, J.M. Characterization of water-sodium alginate dispersions with applications in the food industry. *CYTA-J. Food* **2002**, *3*, 302–306.
25. Tudorache, M.; Bordenave, N. Phenolic compounds mediate aggregation of water-soluble polysaccharides and change their rheological properties: Effect of different phenolic compounds. *Food Hydrocoll.* **2019**, *97*, 105193. [CrossRef]
26. Ocampo, R.D.; Zapateiro, L.A.G.; Gómez, J.M.F.; Torres, C.V. Caracterización bromatológica, fisicoquímica microbiológica y reológica de la pulpa de borojó (*Borojoa patinoi* Cuatrec). *Rev. Cienc. Tecnol.* **2012**, *5*, 17–24. [CrossRef]
27. Tracton, A.A. *Coatings Technology Fundamentals, Testing, and Processing Techniques*; CRC Press Taylor & Francis Group: Boca Raton, FL, USA, 2007; pp. 87–89.
28. Galus, S.; Lenart, A. Development and characterization of composite edible films based on sodium alginate and pectin. *J. Food Eng.* **2013**, *115*, 459–465. [CrossRef]
29. Hernández-Varela, J.D.; Chanona-Pérez, J.J.; Resendis-Hernández, P.; Gonzalez-Victoriano, L.; Méndez-Méndez, J.V.; Cárdenas-Pérez, S.; Calderón-Benavides, H.A. Development and characterization of biopolymers films mechanically reinforced with garlic skin waste for fabrication of compostable dishes. *Food Hydrocoll.* **2022**, *124*, 107252. [CrossRef]
30. Reshmy, R.; Philip, E.; Paul, S.A.; Madhavan, A.; Sindhu, R.; Binod, P.; Pandey, A. A green biorefinery platform for cost-effective nanocellulose production: Investigation of hydrodynamic properties and biodegradability of thin films. *Biomass Convers. Biorefin* **2021**, *11*, 861–870. [CrossRef]
31. Kassab, Z.; Abdellaoui, Y.; Salim, M.H.; Bouhfid, R.; Qaiss, A.E.K.; El Achaby, M. Micro-and nano-celluloses derived from hemp stalks and their effect as polymer reinforcing materials. *Carbohydr. Polym.* **2020**, *245*, 116506. [CrossRef] [PubMed]
32. Xiao, Y.; Liu, Y.; Wang, X.; Li, M.; Lei, H.; Xu, H. Cellulose nanocrystals prepared from wheat bran: Characterization and cytotoxicity assessment. *Int. J. Biol. Macromol.* **2019**, *140*, 225–233. [CrossRef]
33. Kassab, Z.; Abdellaoui, Y.; Salim, M.H.; El Achaby, M. Cellulosic materials from pea (Pisum Sativum) and broad beans (Vicia Faba) pods agro-industrial residues. *Mater. Lett.* **2020**, *280*, 128539. [CrossRef]
34. Ried, K.; Fakler, P. Potential of garlic (*Allium sativum*) in lowering high blood pressure: Mechanisms of action and clinical relevance. *Integr. Blood Press. Control* **2014**, *7*, 71–82. [CrossRef]
35. Kardas, I.; Struszczyk, M.H.; Kucharska, M.; van den Broek, L.A.M.; van Dam, J.E.G.; Ciechańska, D. Chitin and chitosan as functional biopolymers for industrial applications. In *The European Polysaccharide Network of Excellence (EPNOE)*; Navard, E.P., Ed.; Springer: Viena, Austria, 2012; pp. 329–373.
36. Prateepchanachai, S.; Thakhiew, W.; Devahastin, S.; Soponronnarit, S. Mechanical properties improvement of chitosan films via the use of plasticizer, charge modifying agent and film solution homogenization. *Carbohydr. Polym.* **2017**, *174*, 253–261. [CrossRef]
37. Kaya, M.; Khadem, S.; Cakmak, Y.S.; Mujtaba, M.; Ilk, S.; Akyuz, L.; Salaberria, M.; Labidi, J.; Abdulqadir, A.H.; Deligöz, E. Antioxidative and antimicrobial edible chitosan films blended with stem, leaf and seed extracts of *Pistacia terebinthus* for active food packaging. *RSC Adv.* **2018**, *8*, 3941–3950. [CrossRef]
38. Wu, Z.; Li, H.; Ming, J.; Zhao, G. Optimization of adsorption of tea polyphenols into oat β-glucan using response surface methodology. *J. Agric. Food Chem.* **2011**, *59*, 378–385. [CrossRef]
39. Sidek, N.; Manan, N.S.; Mohamad, S. Efficient removal of phenolic compounds from model oil using benzyl Imidazolium-based ionic liquids. *J. Molec. Liq.* **2017**, *240*, 794–802. [CrossRef]
40. Boubakeur, H.; Tanhaş, E.; Erci, F. Alginate-Based Edible Films Loaded by Probiotic and Prebiotic for Preservation of Fresh-Cut Mango Snacks. *Food Bioprocess Technol.* **2026**, *19*, 127. [CrossRef]
41. Kim, S.; Baek, S.K.; Song, K.B. Physical and antioxidant properties of alginate films prepared from *Sargassum fulvellum* with black chokeberry extract. *Food Packag. Shelf Life* **2018**, *18*, 157–163. [CrossRef]
42. Sibaja, B.; Culbertson, E.; Marshall, P.; Boy, R.; Broughton, R.M.; Solano, A.A.; Esquivel, M.; Parker, J.; De La Fuente, L.; Auad, M.L. Preparation of alginate–chitosan fibers with potential biomedical applications. *Carbohydr. Polym.* **2015**, *134*, 598–608. [CrossRef] [PubMed]

43. Al-Sagheer, F.A.; Merchant, S. Visco-elastic properties of chitosan–titania nano-composites. *Carbohydr. Polym.* **2011**, *85*, 356–362. [CrossRef]
44. Kocira, A.; Kozłowicz, K.; Panasiewicz, K.; Staniak, M.; Szpunar-Krok, E.; Hortyńska, P. Polysaccharides as Edible Films and Coatings: Characteristics and Influence on Fruit and Vegetable Quality—A Review. *Agronomy* **2021**, *11*, 813. [CrossRef]
45. Thakhiew, W.; Champahom, M.; Devahastin, S.; Soponronnarit, S. Improvement of mechanical properties of chitosan-based films via physical treatment of film-forming solution. *J. Food Eng.* **2015**, *158*, 66–72. [CrossRef]
46. Peppas, N.A.; Buri, P.A. Surface, interfacial and molecular aspects of polymer bioadhesion on soft tissues. *J. Control. Release* **1985**, *2*, 257–275. [CrossRef]
47. Peppas, N.A.; Sahlin, J.J. Hydrogels as mucoadhesive and bioadhesive materials: A review. *Biomaterials* **1996**, *17*, 1553–1561. [CrossRef] [PubMed]
48. Thakhiew, W.; Devahastin, S.; Soponronnarit, S. Physical and mechanical properties of chitosan films as affected by drying methods and addition of antimicrobial agent. *J. Food Eng.* **2013**, *119*, 140–149. [CrossRef]
49. Agarwal, C.; Kóczán, Z.; Börcsök, Z.; Halász, K.; Pásztory, Z. Valorization of Larix decidua Mill. bark by functionalizing bioextract onto chitosan films for sustainable active food packaging. *Carbohydr. Polym.* **2021**, *271*, 118409. [CrossRef]
50. Kurek, M.; Benbettaieb, N.; Ščetar, M.; Chaudy, E.; Repajić, M.; Klepac, D.; Valic, S.; Debeaufort, F.; Galić, K. Characterization of food packaging films with blackcurrant fruit waste as a source of antioxidant and color sensing intelligent material. *Molecules* **2021**, *26*, 2569. [CrossRef]
51. Carrier, M.; Loppinet-Serani, A.; Denux, D.; Lasnier, J.M.; Ham-Pichavant, F.; Cansell, F.; Aymonier, C. Thermogravimetric analysis as a new method to determine the lignocellulosic composition of biomass. *Biomass Bioenergy* **2011**, *35*, 298–307. [CrossRef]
52. Zhu, F. Polysaccharide based films and coatings for food packaging: Effect of added polyphenols. *Food Chem.* **2021**, *359*, 129871. [CrossRef] [PubMed]
53. Li, X.; Li, F.; Zhang, X.; Tang, W.; Huang, Q.; Tu, Z. Interaction mechanisms of edible film ingredients and their effects on food quality. *Curr. Res. Food Sci.* **2024**, *8*, 100696. [CrossRef]
54. Mugnaini, G.; Bonini, M.; Gentile, L.; Panza, O.; Del Nobile, A.; Conte, A.; Esposito, R.; D'Errico, G.; Moccia, F.; Panzella, L. Effect of design and molecular interactions on the food preserving properties of alginate/pullulan edible films loaded with grape pomace extract. *J. Food Eng.* **2024**, *361*, 111716. [CrossRef]
55. Shahidi, F.; Athiyappan, K.D. Polyphenol-polysaccharide interactions: Molecular mechanisms and potential applications in food systems—A comprehensive review. *Food Prod. Process. Nutr.* **2025**, *7*, 42. [CrossRef]
56. Moreno, L.M.; Gorinstein, S.; Medina, O.J.; Palacios, J.; Muñoz, E.J. Valorization of garlic crops residues as precursors of cellulosic materials. *Waste Biomass Valorization* **2020**, *11*, 4767–4779. [CrossRef]
57. Alzagameem, A.; Khaldi-Hansen, B.E.; Büchner, D.; Larkins, M.; Kamm, B.; Witzleben, S.; Schulze, M. Lignocellulosic Biomass as Source for Lignin-Based Environmentally Bening Antioxidants. *Molecules* **2018**, *23*, 2664. [CrossRef]
58. Wu, S.; Li, G.; Li, B.; Duan, H. Chitosan-based antioxidant films incorporated with root extract of aralia continentalis kitagawa for active food packaging applications. *e-Polymers* **2022**, *22*, 125–135. [CrossRef]
59. Soni, B.; Hassan, E.B.; Schilling, M.W.; Mahmoud, B. Transparent bionanocomposite films based on chitosan and TEMPO-oxidized cellulose nanofibers with enhanced mechanical and barrier properties. *Carbohydr. Polym.* **2016**, *151*, 779–789. [CrossRef]
60. Kulig, D.; Zimoch-Korzycka, A.; Jarmoluk, A.; Marycz, K. Study on Alginate-Chitosan Complex Formed with Different Polymers Ratio. *Polymers* **2016**, *8*, 167. [CrossRef] [PubMed]
61. Singh, R.K.; Patil, T.; Sawarkar, A.N. Pyrolysis of garlic husk biomass: Physico-chemical characterization, thermodynamic and kinetic analyses. *Bioresour. Technol. Rep.* **2020**, *12*, 100558. [CrossRef]

Disclaimer/Publisher's Note: The statements, opinions and data contained in all publications are solely those of the individual author(s) and contributor(s) and not of MDPI and/or the editor(s). MDPI and/or the editor(s) disclaim responsibility for any injury to people or property resulting from any ideas, methods, instructions or products referred to in the content.